Long-Term and Seasonal Patterns in Coastal Temperature and Salinity along the North American West Coast

Franklin B. Schwing

Numerous integrated time series have been assembled that suggest global temperature has been increasing steadily over the last century. One example is the blended series of sea surface temperature (SST) anomalies for the Northern Hemisphere (Folland *et al* 1990). The systematic increase in temperature can be seen at individual locations as well, such as La Jolla, California (Figure 1). However, superimposed on the long-term warming trends of these series are decadal-scale fluctuations, periods of slightly increasing and even decreasing temperature followed by rapid increases in temperature. An alternative view is to interpret this pattern as a series of "regime shifts" (Figure 1), where the mean annual temperature over a short (few year) period makes a rapid shift in response to some environmental stimulus, following a decadal-scale period of relatively level temperature (MacCall and Prager 1988). This regime shift is followed by a long period of relatively level annual temperatures, then another sudden shift back near the previous level.

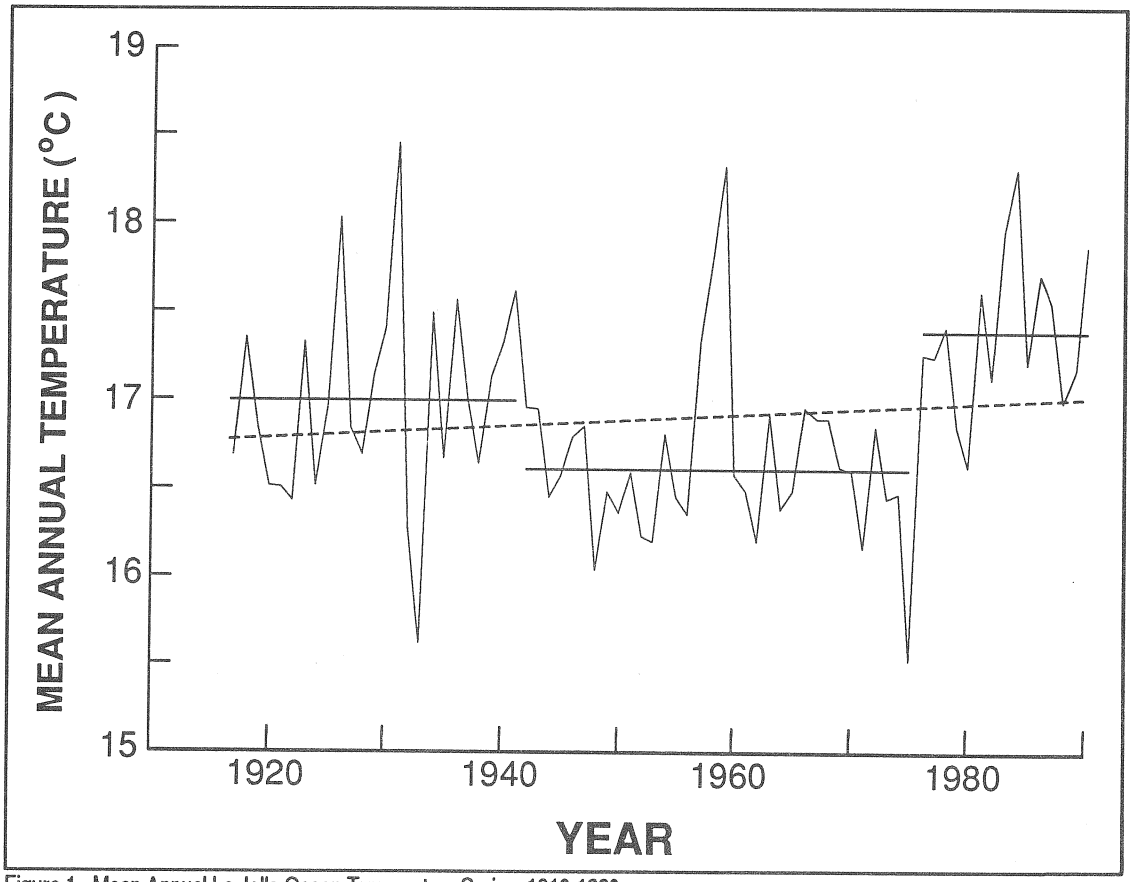

Figure 1. Mean Annual La Jolla Ocean Temperature Series, 1916-1990.
Broken line denotes linear fit to series (0.41°C/100 years, r=0.15).
Solid horizontal lines denote long-term averages shown for three periods: 1916-1941, 1942-1975, 1976-1990.

With either interpretation, we must examine annual-to-decadal fluctuations in SST, define and understand the physical processes responsible for variability on these time scales, and predict the magnitude of temperature change if we are to find the true "climate change" embedded within these individual and composite series. We also must examine regional (sub-ocean basin) spatial scale patterns, because certain areas may be more susceptible to, hence better indicators of, climate change. Regional comparisons also focus more on the ecosystem, where climate change has a biological consequence. Since the physics of ocean regions are generally dominated by one or a few important processes, it is easier to separate out shorter-term patterns from climate effects.

Long monthly-averaged ocean temperature and salinity time series are available from about 40 sites along the North American west coast (Table 1, Figure 2).

Table 1
STATIONS AND PERIODS OF TIME SERIES USED IN THE STATE-SPACE ANALYSIS

Station	Latitude	Longitude	Temperature	Salinity
Seward	60°06'	149°27'	1925-1982	1926-1939
Cape St. James	51°56'	131°01'	1934-1984	1934-1971
Neah Bay	48°22'	124°37'	1935-1986	1936-1979
Crescent City	41°45'	124°12'	1933-1947, 1950-1990	1934-1947, 1950-1979
Bodega Bay	38°19'	123°04'	1957-1990	1975-1990
Farallon Islands	37°25'	122°36'	1925-1942, 1955-1990	1925-1942, 1955-1990
Avila	35°10'	120°45'	1972-1990	
LaJolla	32°52'	117°15'	1916-1990	1916-1990
OS P	50°00'	145°00'	1950-1982	
OS N	30°00'	140°00'	1954-1974	

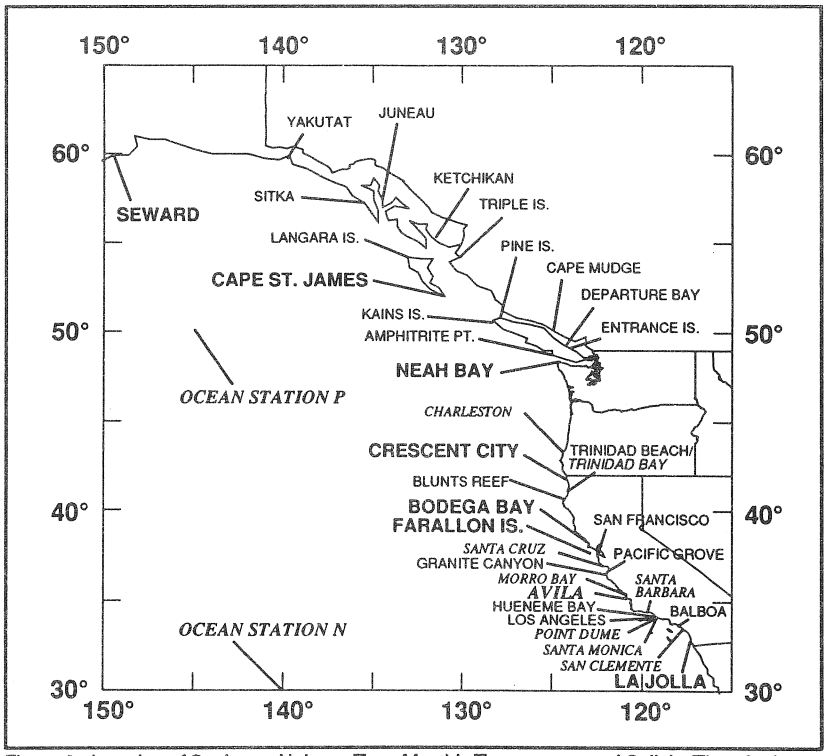

Figure 2. Location of Stations with Long-Term Monthly Temperature and Salinity Time Series.
Sites analyzed in this paper shown in bold. Salinity data not available at italicized stations.

In this pilot study, data for 1931-1990 from eight coastal stations are examined to test the utility of a state-space statistical model (developed by Dr. Roy Mendelssohn, PFEG) in separating and describing seasonal patterns and long-term trends. The stations are: Seward (SE), AK; Cape St. James (CJ), BC; Neah Bay (NB), WA; Crescent City (CC), Bodega Bay (BB), Farallon Is. (FI), Avila (AV), and La Jolla (LJ), CA. These stations were selected based on their series length, their exposure to the ocean, and the extent to which they represent distinct physical regions. For NB, CC, FI, and LJ, long salinity time series are analyzed as well. In addition, temperature from two ocean stations, OSP and OSN, are included to contrast coastal and central ocean sites. For the full study to follow this analysis, all coastal stations will be used. Table 1 shows the location and length of series analyzed here.

Methods

Numerous statistical methods are available to remove "noise" from time series and enhance the signal of interest (*eg*, averaging, spectral filters, spline fits). Normally in smoothing splines,

$$y(t) = T(t) + S(t) + I(t) + E(t) \tag{1}$$

where $y(t)$ is the total signal, $T(t)$ the trend, $S(t)$ the seasonal signal, $I(t)$ the irregular stationary term, and $E(t)$ the error, all at time t. You minimize a term that trades off the goodness of fit to the data with a smoothness constraint, some order of the derivatives are usually zero. Equivalent to smoothing splines, we assume finite differences are constrained. For a smoothness prior, we assume that the series trend, which is made up of the level

$$u(t) - (u(t-1) + b(t-1)) = e_1, N(0, \sigma^2_1) \tag{2a}$$

and slope

$$b(t) - b(t-1) = e_2, N(0, \sigma^2_2), \tag{2b}$$

is equal to a normal random variable N with zero mean and variance σ determined from the constraint that the term be zero. The resulting trend is non-parametric and non-linear. For a first-order trend, on the other hand, Equation 2a,b might be set to zero, giving a linear fit $(y = u + bx)$.

Likewise, for the seasonal term

$$\sum_{\tau=0}^{11} S(t-\tau) = e_3, N(0, \sigma^2_3) \tag{3}$$

we would assume some variance about the zero mean in N. The constraint that Equation 3 equals zero is equivalent to having a stationary seasonal signal; *ie*, each year would be composed of an identical annual curve composed of the averages of the calendar months. Instead, the

seasonal series is non-stationary and non-deterministic. The amplitude, phase and shape of the series can vary over any 12-month period, the mean of which is approximately zero. The non-zero mean of the series is included in the trend. The whole model can be put into state-space form and solved by a combination of Kalman filtering and maximum likelihood, after estimating the variance values initially.

An example of the various series generated by the model is given in Figure 3. The left graph shows the raw monthly La Jolla temperature series, with the trend superimposed in bold. The right graph shows the seasonal and AR (bold) series, plotted on the same scale. It is clear that the trend includes interannual variability, such as ENSOs, and decadal and longer-scale trends. Also note that the trend includes some super-annual variability, which was excluded from the seasonal series due the maximum likelihood calculations.

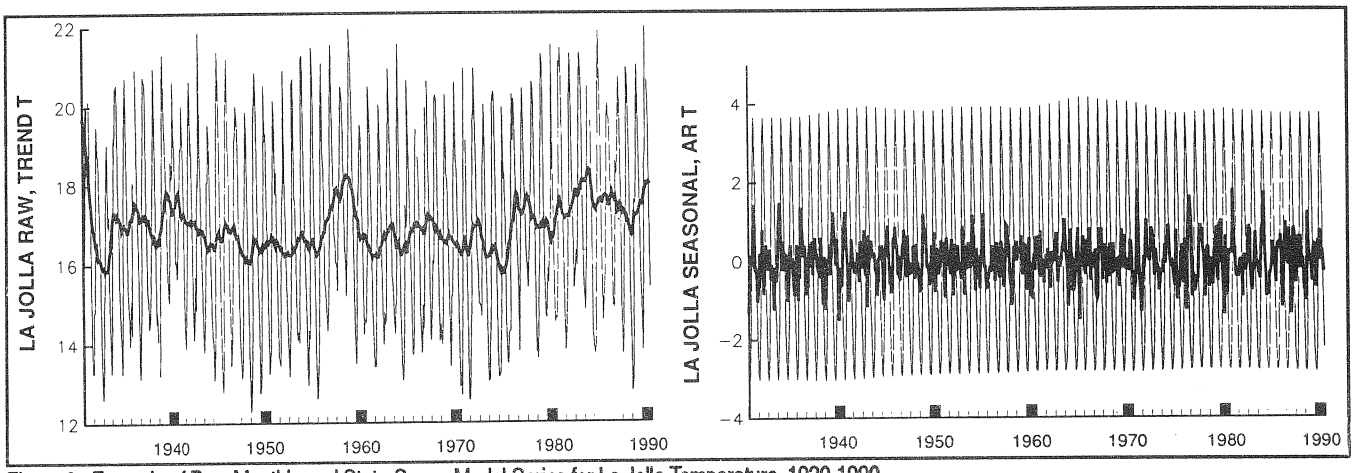

Figure 3. Example of Raw Monthly and State-Space Model Series for La Jolla Temperature, 1930-1990.
Plot at left shows raw and trend model (bold) series; plot at right shows seasonal model and AR (bold) series. Units are in °C.

Seasonal Patterns

I focus first on seasonal patterns, comparing seasonal series at LJ, FI, CC, and NB (Figure 4). Seasonal amplitude was smallest off central California, where coastal upwelling in spring and summer counters seasonal warming. This also resulted in an April temperature minimum and September temperature maximum off central California. Stations off southern California, northwestern United States, Vancouver Island, and Alaska had higher annual amplitudes, with a February minimum and September maximum. Phase shifts in months of temperature maxima and minima caused variations in annual amplitude throughout the series. The secondary maximum in February at FI also fluctuated over time.

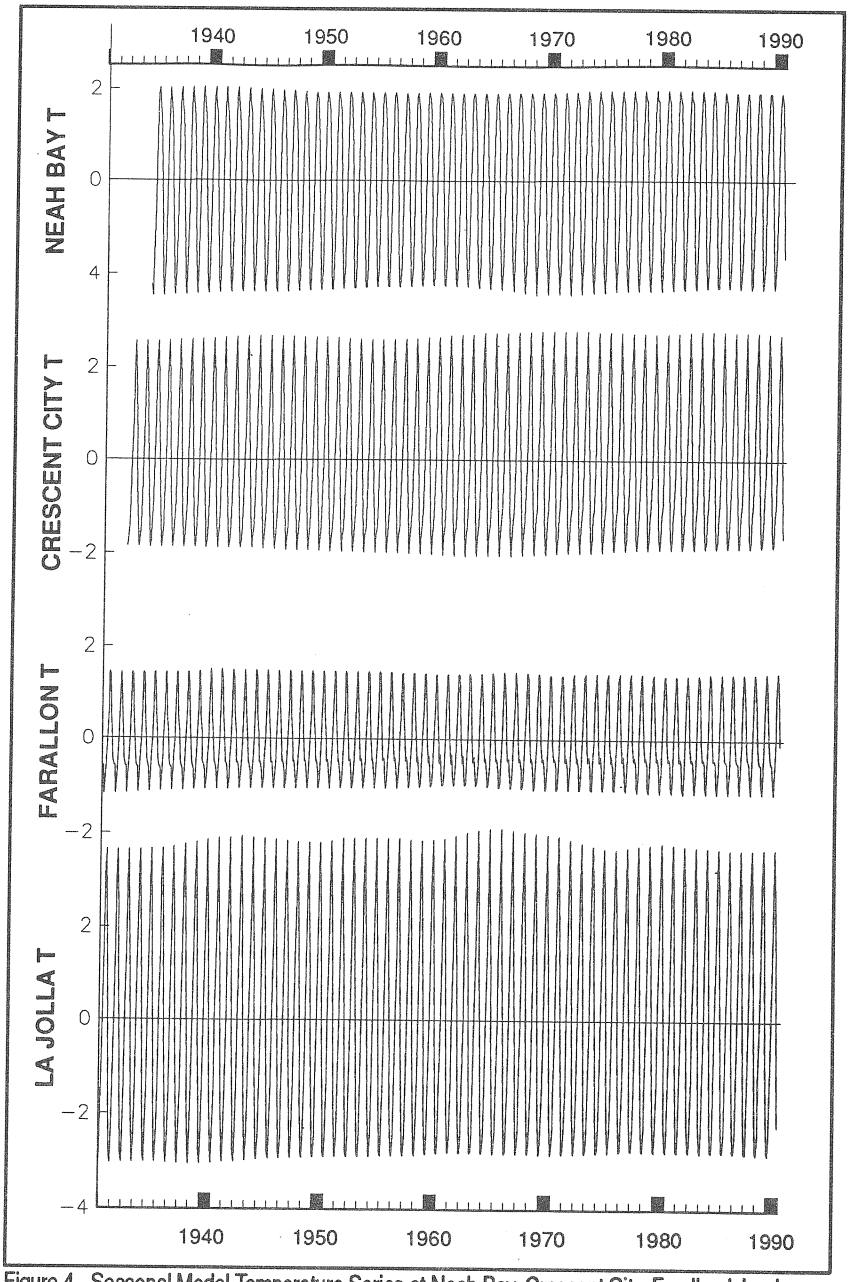

Figure 4. Seasonal Model Temperature Series at Neah Bay, Crescent City, Farallon Islands, and La Jolla, 1930-1990.
Units are in °C.

In contrast, seasonal salinity had its largest amplitude off central California (Figure 5). Compare this to the very small amplitude at LJ (note the change in scale for LJ). At FI, the seasonal salinity minimum was in January/February; the maximum was in June/July. As with temperature, this is related to the importance of seasonal upwelling in this region. Other stations had January minima and August maxima (in phase with temperature). The minimum salinity displays more interannual variability at all sites, due to an upper limit on salinity set by the hydrographic characteristics of each region. Fluctuations in the salinity minimum were due mainly to precipitation and runoff variability.

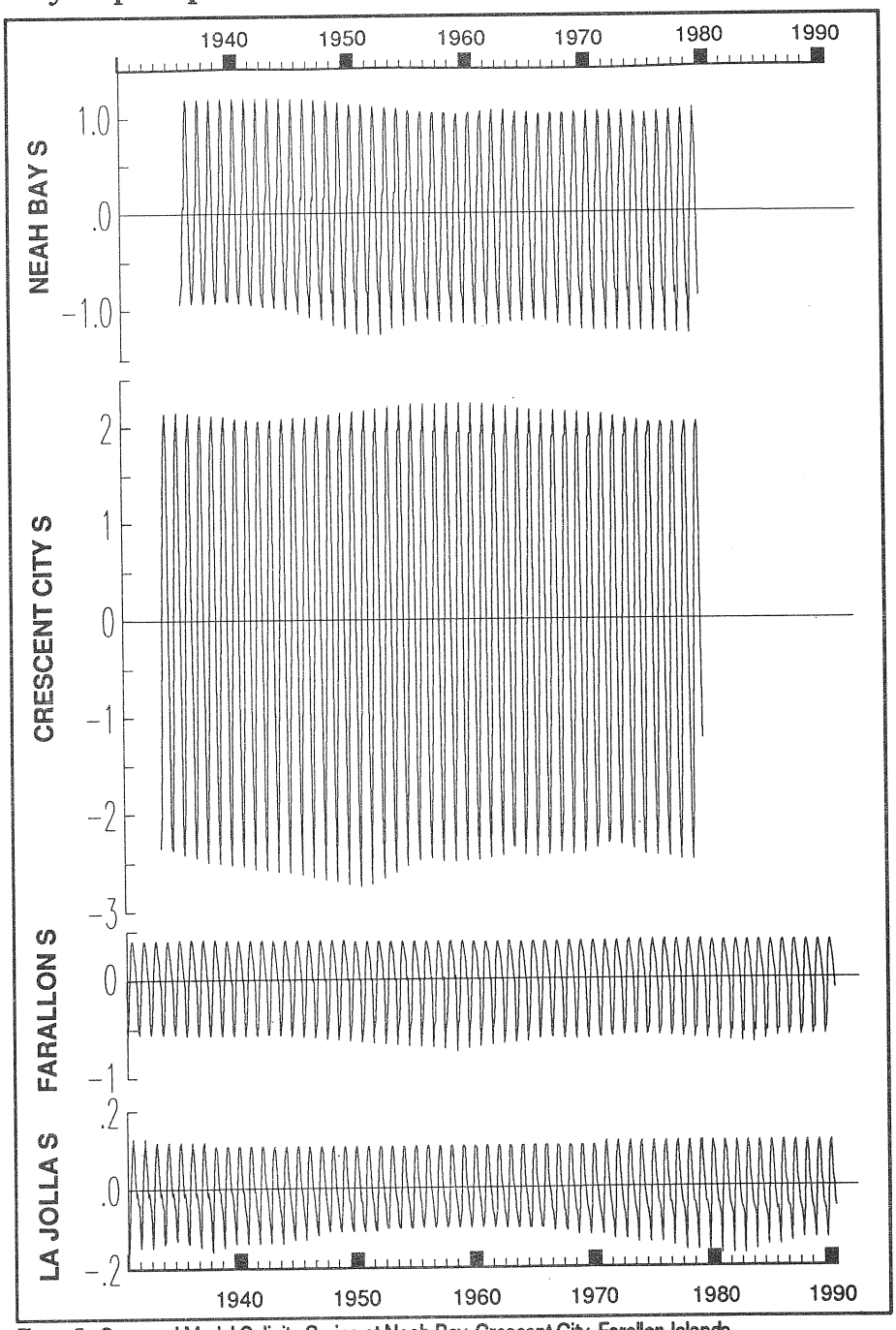

Figure 5. Seasonal Model Salinity Series at Neah Bay, Crescent City, Farallon Islands, and La Jolla, 1930-1990.
Units are parts per thousand.

Again trends in salinity maxima and minima were associated with phase shifts, as well as changes in the magnitude of salinity in each month. At LJ, the lowest salinity minima (*eg*, 1938, 1982) were due to changes in March salinity, such that March values were much less than February at these times but greater than February when the salinity minimum was higher (*eg*, 1960). As with FI seasonal temperature, several stations show secondary salinity maxima and minima, which were due to phase shifts. Seasonal FI salinities in December were normally lower than in November, but December salinities were higher than in November in the late 1950s.

A close-up of FI seasonal temperature and salinity for 1960 to 1980 makes these patterns more apparent (Figure 6). The annual (January to December) signals are not sine curves, as they would be for a series-long annual average; temperature was negative 7 or 8 months each year (December to July). The spring minimum in temperature decreased uniformly from 1960 to 1980 due to a shift in the month of the minimum from April to May. There also was a shift in the maximum from September to October over this period. Generally, February temperatures were greater than January's, resulting in a secondary maximum. The difference in temperature between these months varied from 0.05 to 0.2°C. Near the start and end of the 60-year series (Figure 5), FI temperatures were lower in February than in January. Salinity was in quadrature with temperature at FI, but in phase off northwestern United States and southern California. At FI, salinities were lowest in January (occasionally in February), and greatest in July (occasionally in August). The salinity minimum decreased linearly from 1960 to 1980. Some phase shifting is seen in the winter salinity minimum.

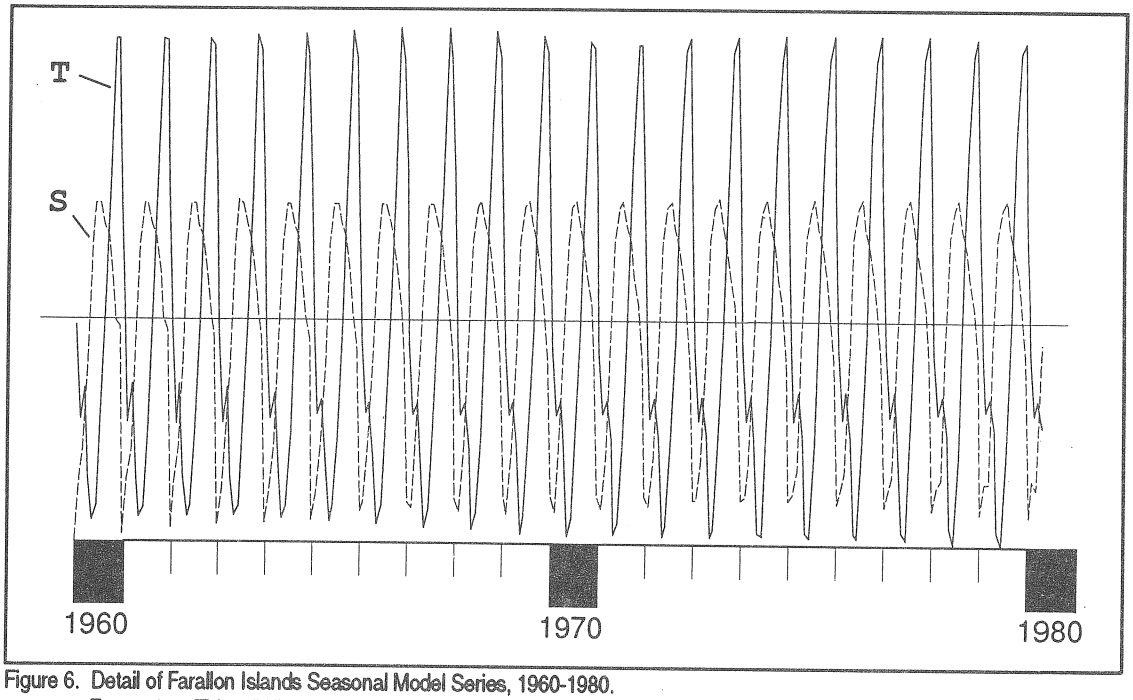

Figure 6. Detail of Farallon Islands Seasonal Model Series, 1960-1980.
Temperature (T) is solid line; salinity (S) is broken line.

Mean temperature and salinity for April to July (the upwelling "season") were calculated in each year from the seasonal model series for LJ, FI, CC, and NB (Figure 7). Except for LJ, all April-July seasonal temperature series decreased with time and all salinity series increased with time, implying increased upwelling. Magnitude of the changes was about 0.05-0.1°C and 0.1ppt over 60 years. Correlations versus time are highly significant. Changes in April-July temperature and salinity are not linear over time; certain years stand out as times of substantial change in slope (*eg*, 1943, 1963-1965). Regressions of temperature against salinity *(T/S)* at NB, CC, and FI are highly significant and negative, consistent with the *T/S* upwelling relationship. The *T/S* LJ slope is positive and not statistically significant, implying multidecadal changes in upwelling are not a factor here. This is consistent with the fact that during these months, upwelling is a dominant process off northern and central California but not near LJ. A next step is to determine if variations in other environmental series (*ie*, wind, sea level) are linked to these fluctuations.

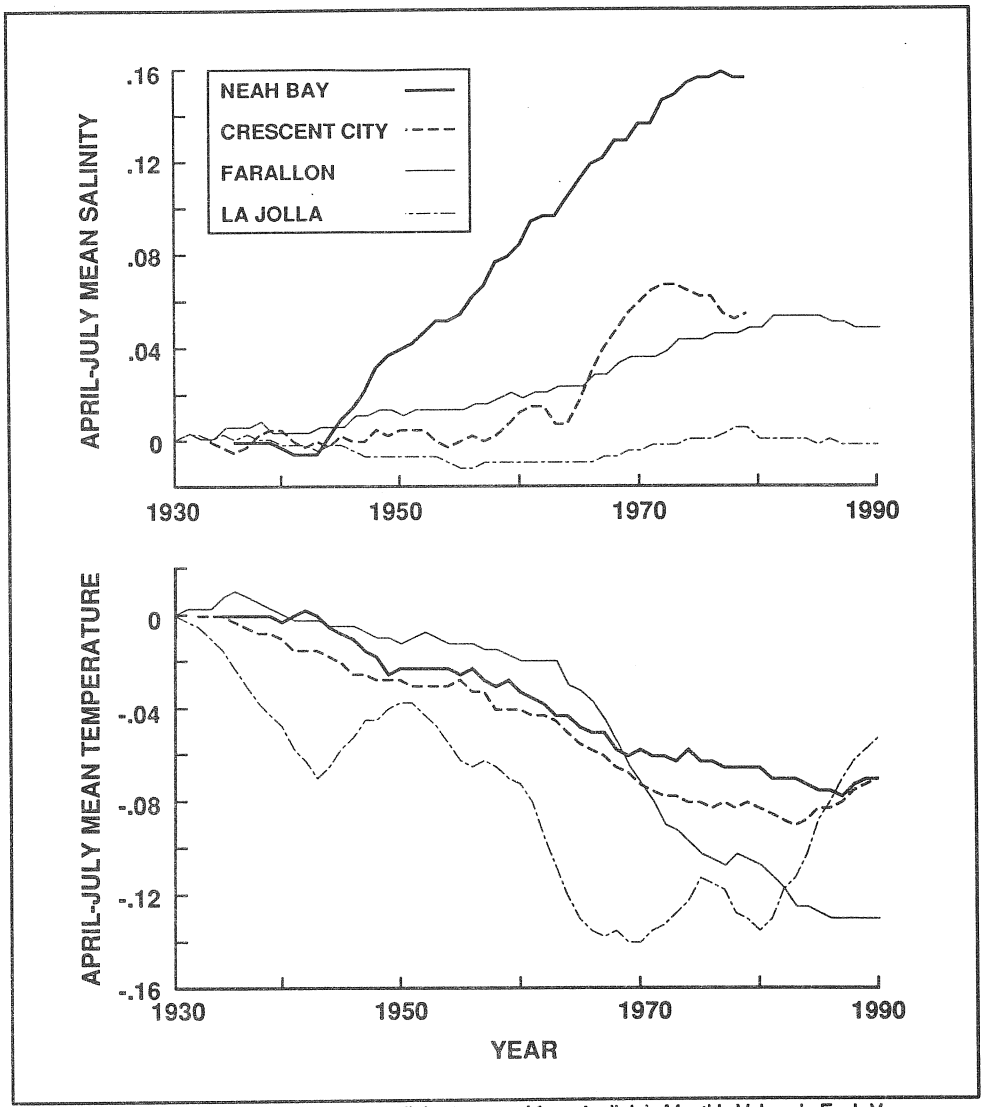

Figure 7. Time Series of Temperature and Salinity Averaged from April-July Monthly Values in Each Year, Derived from Seasonal Model Series, for Neah Bay, Crescent City, Farallon Islands, and La Jolla. Units are °C for temperature and parts per thousand for salinity.

Regression slopes of April-July temperature and salinity from the raw FI series against time are of the same signs as for the seasonal series (temperature negative, salinity positive) but not statistically significant (Table 2). Slopes in similar series derived from the model trend data are opposite (temperature positive, salinity negative) and less well correlated. Evidence for increased upwelling cannot be seen in the trend series, which are analogous to averaged, smoothed, or low-pass-filtered series. The FI April-July trend slopes and r values for temperature and salinity are virtually identical to those for the annual averages, implying that seasonal effects of upwelling do not occur in the trend series. The raw FI annual averages are the same sign as these, but opposite the sign of the April-July raw averages. Changes in temperature and salinity due to upwelling are an order of magnitude lower than the climate change variations in these series, and they are confined to spring and summer and, thus, are dwarfed by the trends of increasing temperature and decreasing salinity (at FI) in the raw observations.

Table 2
SLOPE OF LINEAR FIT AND CORRELATION (r) BETWEEN AVERAGE FARALLON ISLANDS TEMPERATURE AND SALINITY VERSUS YEAR, DETERMINED FROM SEASONAL AND TREND MODEL SERIES AND FROM RAW MONTHLY-AVERAGE TIME SERIES

NS denotes r is not significant at the 0.05 level.
April-July refers to yearly averages for those months; 12 month refers to yearly averages for all months.

		Temperature		Salinity	
		Slope (°C/year)	r	Slope (ppt/year)	r
Seasonal	(April-July)	-0.0027	-0.94	0.0010	0.97
Trend	(April-July)	0.0159	0.30	-0.0111	-0.28
	(12 month)	0.0179	0.33	-0.0127	-0.29
Raw	(April-July)	-0.0075	-0.15(NS)	0.0037	0.22(NS)
	(12 month)	0.0100	0.26(NS)	-0.0023	-0.24(NS)

Examination of other stations reveals similar patterns. AV, BB, and OSN all show a net decrease in April-July temperature over the length of the seasonal series, counter to the temperature increase in the trend series at these sites. In contrast, OSP temperature increased over this period. Stations north of 50°N show no steady pattern in April-July temperature.

Phase shifts in the coastal series may be related to temporal shifts in wind stress or large-scale current patterns (*eg*, California Undercurrent/ Davidson Current). A time series of yearly averages of monthly estimates of April-September alongshore wind stress off California (Bakun 1990) shows a statistically significant increase over time, corresponding to an increase in upwelling intensity. The series trend agrees with that at other latitudes along the western North American coast and other coastal upwelling regions. Thus, there may be a relationship between long-term increases in wind stress and coastal upwelling rates along the west coast, which would be most obvious during spring and summer. Further analysis of coastal wind, temperature, salinity, and sea level series is needed to clarify this relationship.

Trend Series

Trend model series for the eight coastal sites examined, plus OSN and OSP, are presented in Figure 8. Temperature series are offset, relative to Seward, by the amount (°C) shown in parentheses. Note that the model fits a trend through missing observations. Some of these periods are apparent (*eg*, FI in 1943-1954). Major ENSO events (Quinn *et al* 1987) are shown with the darker shaded vertical lines; moderate ENSO years

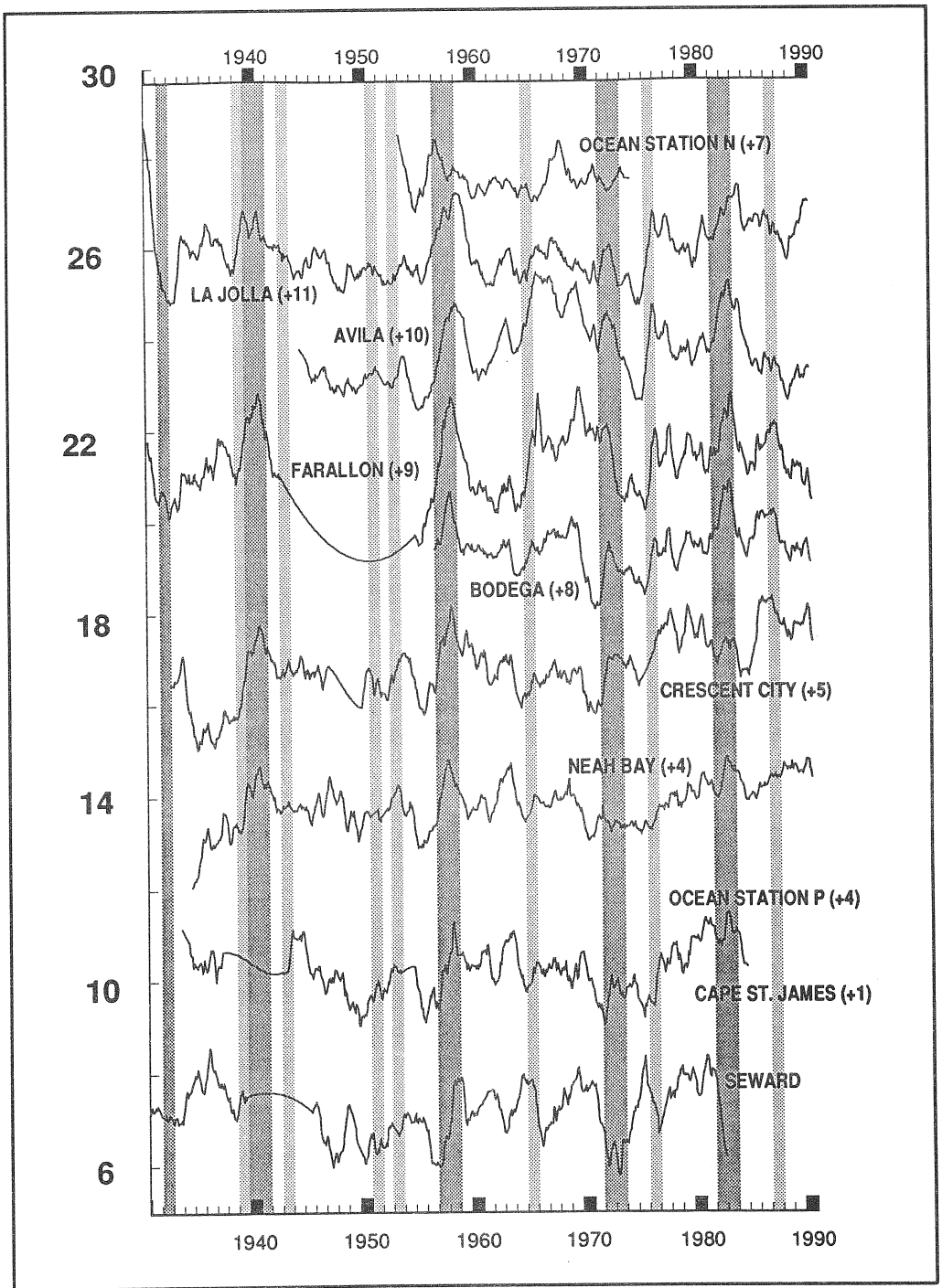

Figure 8. Trend Model Series for Temperature, 1930-1990.
Values in parentheses denotes vertical offset of series, in °C, relative to Seward. Darker shaded vertical lines show major ENSO events; lighter shaded vertical lines show moderate ENSO events, based on Quinn *et al* (1987).

are noted by lighter shaded lines. Large-scale warming effects of ENSOs are seen. Some ENSO events (*eg*, 1973) appear to be constrained to southern stations.

Numerous other regional differences in the trends are evident. Most sites have series-length warming trends that are highly non-linear and display considerable variability on annual/decadal scales. Most series have 10- to 20-year periods of relatively level temperature, followed by 10- to 20-year periods of rapid temperature increase. Some series have multi-year periods of decreasing temperature. Interannual variation on a 2-year period is seen frequently at most sites, possibly the Quasi-Biennial Oscillation (CD Keeling, pers comm).

Finally consider the suggested shifts to a cool regime in 1941 and to a warm regime in 1975 (Figure 1). The 1975 shift occurs rapidly at LJ and AV. At sites farther north, shifts are less dramatic and occur over several years, appearing more as gradual transitions than sudden shifts. The cool shift in 1941 is more difficult to document and appears less dramatic at LJ relative to the 1975 shift. The regime shift concept may be valid for some regions (*eg*, southern California), but it has a considerable degree of inter-regional difference. Keep in mind that series presented here are model trends derived from the monthly values of temperature (12/year) with the seasonal patterns removed, very different from those in Figure 1, which are annual averages (1/year). Future studies should focus on what mechanisms may be responsible for such shifts (*eg*, ENSO), and how the effect spreads along the coast (*ie*, a sudden shift off southern California that "diffuses" northward).

The salinity trend series (LJ, FI, CC, NB) show even larger regional differences (Figure 9). Large fluctuations are correlated visually to the PACLIM freshwater runoff series (Cayan et al 1988); *ie*, NB to Puget Sound (about 1945), CC to Columbia River, FI to San Francisco Bay. Lack of significant freshwater input near LJ may be responsible for the relatively small variations there. ENSOs are evident as lower salinity, presumably due to greater runoff associated with higher rainfall. The most outstanding features in LJ salinity are the sudden drops in 1941 and 1976, coincident with the regime shifts. This suggests that large-scale changes in current patterns, which probably dominate water characteristics at LJ, may be linked to such shifts.

Bakun (1990) noted a significant increase in April-September alongshore wind stress off California. However, the pattern reversed in the mid-1970s toward decreasing wind stress, corresponding to the increase in the temperature trend series, especially that at LJ. Thus, there is a potential link between "regime shifts" in wind and temperature. It will be enlightening to apply the state-space model to the wind series analyzed by Bakun, and compare upwelling trend and seasonal model series for wind to patterns in the ocean temperature model series described here.

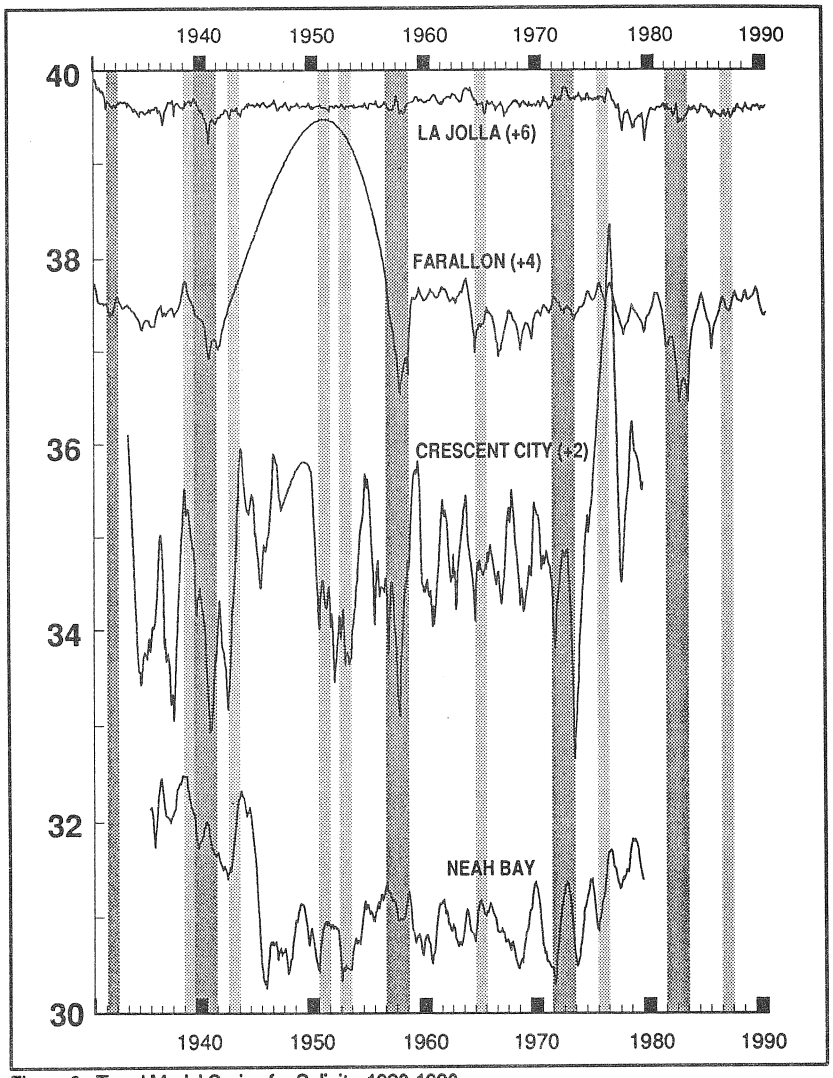

Figure 9. Trend Model Series for Salinity, 1930-1990.
Values in parentheses denotes vertical offset of series, in ppt, relative to Seward.
Darker shaded vertical lines show major ENSO events; lighter shaded vertical lines show moderate ENSO events, based on Quinn *et al* (1987).

Table 3 shows correlations *(r)* between various trend model series. Values in the upper-right half of the matrix are correlations between temperature for the ten stations. The sparse lower-left portion of the matrix shows r values representing salinity at four sites (LJ, FI, CC and NB). Underlined values on the diagonal are correlations between temperature and salinity at those four sites. Because the series have different lengths, the number of observations *(n)* differs for various pairings *(n=252(w/OSN)-720)*. Correlations that are not statistically significant (0.05 level) are italicized. Correlations between temperature at most stations are significant, probably due to ENSOs and interannual events (large-scale processes); all are positive. LJ temperature is particularly well correlated with other sites. Seward and OSN temperatures are generally uncorrelated with other series. Correlations between temperature series are greater than between salinity series, and the sign for salinity is not consistent. A strong negative *T/S* correlation is seen at FI; the other three *T/S* correlations are smaller. Of the four sites examined, only CC has a positive *T/S* correlation.

Table 3
CORRELATIONS BETWEEN COASTAL STATION TEMPERATURE AND SALINITY TREND SERIES

Upper-right diagonal shows r values between temperature series.
Lower-left diagonal shows r between salinity series for Neah Bah, Crescent City, Farallon Islands, and La Jolla.
Correlations between temperature and salinity at these four sites are underlined.
Correlations not statistically significant (0.05 level) are italicized.

	Correlations Between Shore Stations								
	SE	CJ	NB	CC	BB	FI	AV	LJ	OSN
OS P	0.14	0.57	0.54	0.64	0.47	0.22	*0.08*	0.43	0.21
Seward	==	0.44	*0.01*	*0.01*	*0.01*	0.42	0.23	0.19	*-0.08*
Cape St. James		==	0.52	0.39	0.70	0.42	0.47	0.52	*0.05*
Neah Bay			-0.17	0.76	0.67	0.30	0.23	0.50	0.31
Crescent City			*0.06*	0.17	0.58	0.34	0.10	0.49	0.34
Bodega Bay				==		0.55	0.37	0.66	0.24
Farallon Islands			-0.35	0.17		-0.86	0.56	0.73	*0.10*
Avila							==	0.43	*0.08*
La Jolla			-0.34	0.22		0.14		-0.16	0.35

With the exception of OSP (Table 4), linear fits to all coastal temperature trend series versus time have positive slopes and, except for the two northernmost stations and OSN, are statistically significant (despite the considerable non-linear shape of the series). The greatest slopes are seen off northern and central California, despite the fact that the standard deviations

Table 4
ESTIMATES OF LINEAR FITS TO TEMPERATURE AND SALINITY TREND SERIES AGAINST TIME

r denotes correlation between series and time.

Temperature				
	Series Mean (°C)	Linear Slope (°C/yr)	Standard Deviation of Slope (°C/yr)	r
Seward	7.22	0.0015	0.0015	0.04
Cape St. James	9.26	0.0024	0.0014	0.07
Neah Bay	9.84	0.0136***	0.0010	0.45***
Crescent City	11.84	0.0244***	0.0012	0.60***
Bodega Bay	11.45	0.0070**	0.0025	0.14**
Farallon Islands	11.97	0.0179***	0.0019	0.33***
Avila	13.75	0.0132***	0.0022	0.24***
La Jolla	16.94	0.0060***	0.0013	0.18***
OS P	8.25	0.0048*	0.0024	0.10*
OS N	20.53	-0.0060	0.0034	-0.11

Salinity				
	Series Mean (ppt)	Linear Slope (ppt/year)	Standard Deviation of Slope (ppt/year)	r
Neah Bay	31.17	-0.0174***	0.0017	-0.41***
Crescent City	30.81	0.0220***	0.0026	0.34***
Farallon Islands	33.72	-0.0117***	0.0014	-0.29***
La Jolla	33.60	-0.0005**	0.0002	-0.10**

* P<0.05
** P<0.01
*** P<0.0001

of slopes are similar in all regions. The FI temperature slope is three times that for the LJ series for the common 60-year period analyzed here, so differences in the series length do not necessarily account for the differences in slope. It is obvious, however, that because of the substantial decadal swings in temperature and salinity (Figures 8 and 9), analysis of different length series could provide very different linear fits. For salinity, the LJ slope and standard deviation is much smaller than the others. The slope for CC salinity versus time is positive; NB, FI, and LJ are negative.

Summary

The state-space model appears to be a powerful tool in separating interannual-to-interdecadal fluctuations in environmental time series from seasonal patterns of variability. Further testing of the method on additional time series will provide a better indication of its applicability and, hopefully, a more thorough understanding of the linkages between long-term variations in atmospheric forcing and the coastal ocean's response to this variability, as well as the potential contribution of natural and anthropogenic signals, and regional differences in these effects. Results presented here demonstrate the importance of evaluating temporal and spatial variability over the entire spectrum, rather than simply at global climate scales, when examining long-term environmental fluctuations.

The results show a clear separation of the non-stationary seasonal signal from the non-linear trend for coastal ocean temperature and salinity. Overall, the temperature trend series are highly correlated with each other. Superimposed on a general, statistically significant pattern of increasing temperature are significant fluctuations on annual-decadal scales (*eg*, ENSO, "regime shifts"), as well as substantial regional differences in the rate of warming and in the degree to which interannual events affect the overall trend. Salinity trends are more ambiguous but appear to be linked to regional differences in freshwater runoff and possibly changes in ocean circulation.

Like the trend series, significant regional differences were found in the seasonal series. The utility of estimating non-stationary seasonal patterns is demonstrated with the finding of a systematic decrease in temperature and increase in salinity during spring and summer, evidence that coastal upwelling is increasing in intensity. This pattern cannot be discerned in the trend series and is not statistically significant in the raw observations. It also is most prevalent in areas where seasonal upwelling is a major process. Shifts in the phase and amplitude of the seasonal cycle over several decades are suggested with this technique as well.

In future studies, the entire set of coastal temperature and salinity data will be incorporated with series of wind and sea level observations to examine the relationship between atmospheric and oceanic variables. The model will be updated to derive separate estimates of trend and

seasonal series common to the entire set (*ie*, the "global" signal), in contrast to those unique to regions or even individual sites. This will provide a better contrast between truly global/climate changes and regional/ecosystem level environmental fluctuations. The addition of other model terms to estimate the role of phenomena such as ENSO and the QBO will be considered as well.

Acknowledgments

The author greatly acknowledges Dr. Roy Mendelssohn, PFEG, Monterey, California, for his assistance and expertise in development and application of the state-space model. Data used in the analysis were supplied by Dr. John McGowan and Pat Walker, MLRG, Scripps Institution of Oceanography, La Jolla, California, and obtained from the PACLIM Time Series Data Base. I also thank Dr. Dave Keeling, SIO, for his provocative comments following the presentation of these results at the PACLIM '93 Workshop.

References

Bakun, A. 1990. Global Climate Change and Intensification of Coastal Ocean Upwelling. *Science.* 247:198-201.

Bottomley, M, CK Folland, J Hsiung, RE Newell, DE Parker. 1990. *Global Ocean Surface Temperature Atlas (GOSTA).* Joint Met. Office/Massachusetts Institute of Technology Project. 20+iv pp and 313 plates. HMSO, London.

Cayan, DR, DR McLain, WD Nichols, JS DiLeo-Stevens. 1988. *Monthly Climatic Time Series Data from the Pacific Ocean and Western Americas.* USGS Open-File Report. 379 pp.

Folland, CK, TR Karl, KY Vinnikov. 1990. Observed Climate Variations and Change. Pages 195-238 in *Climate Change, the IPCC Scientific Assessment.* JT Houghton, GJ Jenkins, JJ Ephraums (editors). WMO/UNEP/IPCC. Cambridge University Press.

Jones, PD, TML Wigley, G Farmer. 1991. Marine and Land Temperature Sets: a Comparison and a Look at Recent Trends. Pages 153-172 in *Greenhouse-Gas-Induced Climatic Change: a Critical Appraisal of Simulations and Observations.* ME Schlesinger (editor) Elsevier, Amsterdam.

MacCall, AD, and MH Prager. 1988. Historical Changes in Abundance of Six Fish Species Off Southern California, Based on CalCOFI Egg and Larva Samples. *CalCOFI Reports.* 29:91-101.

Quinn, WH, VT.Neal, SE Antunez de Mayolo. 1987. El Niño Occurrences over the Past Four and a Half Centuries. *Journal of Geophysical Research.* 92:14,449-14,461.